ELSEVIER

Journal of Quantitative Spectroscopy & Radiative Transfer 101 (2006) 488–497

Journal of Quantitative Spectroscopy & Radiative Transfer

www.elsevier.com/locate/jqsrt

Modeling single-scattering properties of small cirrus particles by use of a size-shape distribution of ice spheroids and cylinders

Li Liu[a,b], Michael I. Mishchenko[b,*], Brian Cairns[a,b], Barbara E. Carlson[b], Larry D. Travis[b]

[a]*Department of Applied Physics and Applied Mathematics, Columbia University, 2880 Broadway, New York, NY 10025, USA*
[b]*NASA Goddard Institute for Space Studies, 2880 Broadway, New York, NY 10025, USA*

Abstract

In this study, we model single-scattering properties of small cirrus crystals using mixtures of polydisperse, randomly oriented spheroids and cylinders with varying aspect ratios and with a refractive index representative of water ice at a wavelength of 1.88 μm. The Stokes scattering matrix elements averaged over wide shape distributions of spheroids and cylinders are compared with those computed for polydisperse surface-equivalent spheres. The shape-averaged phase function for a mixture of oblate and prolate spheroids is smooth, featureless, and nearly flat at side-scattering angles and closely resembles those typically measured for cirrus. Compared with the ensemble-averaged phase function for spheroids, that for a shape distribution of cylinders shows a relatively deeper minimum at side-scattering angles. This may indicate that light scattering from realistic cirrus crystals can be better represented by a shape mixture of ice spheroids. Interestingly, the single-scattering properties of shape-averaged oblate and prolate cylinders are very similar to those of compact cylinders with a diameter-to-length ratio of unity. The differences in the optical cross sections, single-scattering albedo, and asymmetry parameter between the spherical and the nonspherical particles studied appear to be relatively small. This may suggest that for a given optical thickness, the influence of particle shape on the radiative forcing caused by a cloud composed of small ice crystals can be negligible.

Keywords: Cirrus clouds; Scattering; Remote sensing; Atmospheric radiation

1. Introduction

Cirrus clouds play an important role in the earth–atmosphere radiation balance [1]. They modulate atmospheric radiation by trapping outgoing infrared radiation and by reflecting and absorbing incoming short-wave solar radiation. However, cirrus clouds remain a significant source of uncertainty in climate modeling, partly due to our incomplete knowledge of the microphysical and radiative properties of cirrus. This lack of understanding is largely caused by cirrus being generally composed of nonspherical ice particles [1,2].

*Corresponding author. Tel.: +1 212 678 5590; fax: +1 212 678 5622.
E-mail address: crmim@giss.nasa.gov (M.I. Mishchenko).

0022-4073/$ - see front matter © 2006 Elsevier Ltd. All rights reserved.
doi:10.1016/j.jqsrt.2006.02.040

The calculated radiative impact of cirrus clouds on climate is affected by a choice of the theoretical scattering phase function or by derived parameters such as the asymmetry parameter g, which are poorly known [3]. The knowledge of the angular scattering behavior of atmospheric ice particles is even more important in the development of reliable remote-sensing techniques for the detection of cirrus clouds and the retrieval of their optical and microphysical properties [4,5]. It has been shown that the use of an incorrect phase function can lead to significant errors in the retrieval of the cloud optical thickness and microphysical properties [2,5,6].

Many observations of cirrus clouds indicate that typical ice crystal phase functions are rather smooth and featureless [2,3,7–10]. This smooth scattering-angle dependence can be explained, at least partially, by natural particle ensembles being mixtures of different shapes in which shape-specific details of individual phase functions are averaged out [5,11–13]. Indeed, observations for mid-latitude, tropical, and contrail cirrus show that these clouds can exhibit a great variety of particle habits [14]. At present, there is no technique available for the accurate computation of light scattering by nonspherical ice crystals covering the entire range of sizes and shapes that can occur in cirrus clouds and contrails. Although the scattering and radiative properties of particles much greater in size than a wavelength may be adequately represented by the geometrical optics technique, the calculation of the optical properties of nonspherical particles with size parameters (ratio of particle circumference to wavelength of observation) less than about 200 [15] remains a difficult task [16,17]. This theoretical limitation is especially unfortunate in view of the accumulating evidence that a significant fraction of ice crystals have sizes significantly smaller than those assumed in most current climate models. It is, therefore, highly desirable to find a simple and yet sufficiently accurate theoretical method to model single scattering by an ensemble of natural nonspherical ice crystals with sizes ranging from 0 to $\sim$10 μm (see, e.g., [18–25]).

Back in the 1980s, Hill et al. [26] used axially symmetric spheroids in order to represent scattering from an ensemble of natural nonspherical soil particles. Mishchenko et al. [13] also modeled phase functions for dustlike tropospheric aerosols using a shape mixture of randomly oriented oblate and prolate polydisperse spheroids in random orientation. They concluded that although natural dust particle ensembles are typically mixtures of irregular shapes, their cumulative phase function can be adequately modeled using a wide aspect-ratio distribution of prolate and oblate spheroidal grains. More recently, Xu et al. [27], Baran [28], Lee et al. [29], and Kahn et al. [30] modeled scattering from cirrus at infrared wavelengths by using a distribution of circular ice cylinders of different sizes and shapes.

Encouraged by these recent studies as well as by the results of [31–37], we use the statistical approach outlined in [12,13,26] to model the optical cross sections and the elements of the Stokes scattering matrix for small cirrus cloud particles. The main motivation for this research stems from the need to develop cirrus retrieval algorithms based on multi-spectral and multi-angle radiance and polarization observations and apply them to data collected with the Research Scanning Polarimeter (RSP) [38] and the Glory Aerosol Polarimetry Sensor (APS) [39].

2. Computations

We first computed light scattering by polydisperse randomly oriented oblate and prolate spheroids with aspect ratios varying from 1.2 (nearly spherical particles) to 2.4 (highly aspherical particles) in steps of 0.2 using the highly efficient T-matrix code [17] publicly available on the World Wide Web at http://www.giss.nasa.gov/~crmim. Similarly, we modeled single scattering by polydisperse randomly oriented oblate and prolate cylinders with diameter-to-length ratios D/L or length-to-diameter ratios L/D varying from 1.2 to 2.4 in steps of 0.2. We then computed the cumulative optical cross sections and the Stokes scattering matrices for shape mixtures of polydisperse spheroids and cylinders using the formulas provided by Mishchenko et al. [13]. In this study, we have adopted the modified power law size distribution given by [17]

$$n(r) = \begin{cases} C & \text{for } r \leqslant r_1, \\ C(r_1/r)^3 & \text{for } r_1 \leqslant r \leqslant r_2, \\ 0 & \text{for } r \geqslant r_2, \end{cases} \tag{1}$$

where C is a normalization constant and r is the surface-equivalent-sphere radius. The parameters r_1 and r_2 are chosen such that the effective radius of the size distribution, r_{eff}, is equal to 5 μm and the effective variance, v_{eff}, is fixed at 0.2, thereby representing a moderately wide distribution [40]. An important practical advantage of the modified power law size distribution is that for the same v_{eff}, it has a much smaller value of the maximal radius r_2 than optically equivalent gamma and log normal distributions, thereby significantly accelerating computer computations. It is noted that the r_{eff} value used in this study is consistent with those inferred in [18–25].

We calculated light scattering by model cirrus particles at a wavelength of 1.88 μm, which is the nominal wavelength of one of the RSP spectral channels. The corresponding real and imaginary parts of the refractive index of ice are 1.2788 and 0.000317, respectively. The wavelength 1.88 μm represents a spectral channel quite suitable for remote sensing of cirrus since it is effectively screened from the surface by water vapor absorption and only probes the upper troposphere. It is therefore used on both the MODIS Airborne Simulator and the RSP instrument for detection and characterization of thin cirrus clouds. A similar channel centered at the 1.37 μm water vapor absorption band has been selected for both RSP and APS as well as for a nearly identical instrument to be flown by the US National Polar-Orbiting Operational Environmental Satellite System (NPOESS) program (http://www.ipo.noaa.gov/Technology/aps_summary.html).

3. Results and discussion

Fig. 1 shows the elements of the normalized Stokes scattering matrix (as defined in Section 4.10 of [17]) averaged over all oblate (dotted curves) and prolate (dashed curves) spheroids with aspect ratios ranging from 1.2 to 2.4 in steps of 0.2. The comparison of the single-scattering characteristics with those for surface-equivalent polydisperse spherical particles (solid curves) indicates that the scattering properties of natural ice particles may be significantly different from those of equivalent ice spheres. The ensemble-averaged phase functions for oblate and prolate spheroidal particles, depicted, respectively, by the dotted and dashed curves, are rather smooth and lie close to each other despite the fact that they are computed for spheroids of quite different shapes. This result reinforces the conclusion that the phase function of a representative shape mixture of nonspherical particles can be fairly insensitive to which elementary shapes are used to form the mixture [13]. The relative differences in other scattering matrix elements between shape-averaged oblate and prolate spheroids are more significant compared with those of the phase functions.

Similar to Fig. 1, Fig. 2 presents the elements of the normalized Stokes scattering matrix for polydisperse spheres (solid curves), for compact cylinders with a diameter-to-length ratio $D/L = 1$ (dotted curves), and for equiprobable shape mixtures of oblate (dashed curves) and prolate cylinders (dash-dotted curves) with the values of D/L or L/D ranging from 1.2 to 2.4 in steps of 0.2. Again, we can see large differences between the curves for polydisperse spheres and cylinders. Interestingly, the single-scattering properties of polydisperse, randomly oriented compact cylinders shown by the dotted curves are rather close to those of the shape mixture of oblate and prolate cylinders, especially for the phase function a_1, the polarization ratio $-b_1/a_1$, and the element ratio b_2/a_1. A possible implication of this result is that one can simplify the computation of light scattering by an ensemble of cylinders with a wide distribution of aspect ratios by calculating the single-scattering characteristics for compact cylinders. This is not unrealistic since experimental errors may often exceed the magnitude of the theoretical differences for these classes of particles.

It should be noted that, in general, spheroids exhibit a much stronger variability of the scattering properties with aspect ratio than circular cylinders, as revealed by Figs. 3 and 4. This conclusion has already been drawn by Mishchenko et al. [41], who studied light scattering by circular cylinders with a refractive index typical of mineral dust. This strong variability appears to make spheroids more suitable than cylinders when one attempts to reproduce laboratory data for natural irregular particles by varying the composition of a shape mixture of simple nonspherical shapes. It is interesting to note that the results of Nousiainen et al. [37] suggest that spheroids appear to have a similar advantage over low-symmetry particles in the form of polyhedral prisms.

Fig. 5 shows the normalized scattering matrix for polydisperse spheres (solid curves) and for equiprobable shape mixtures of all spheroids (oblate and prolate spheroids) and cylinders (oblate and prolate cylinders), depicted by the dotted and dashed curves, respectively. It is seen that the phase function averaged over a wide

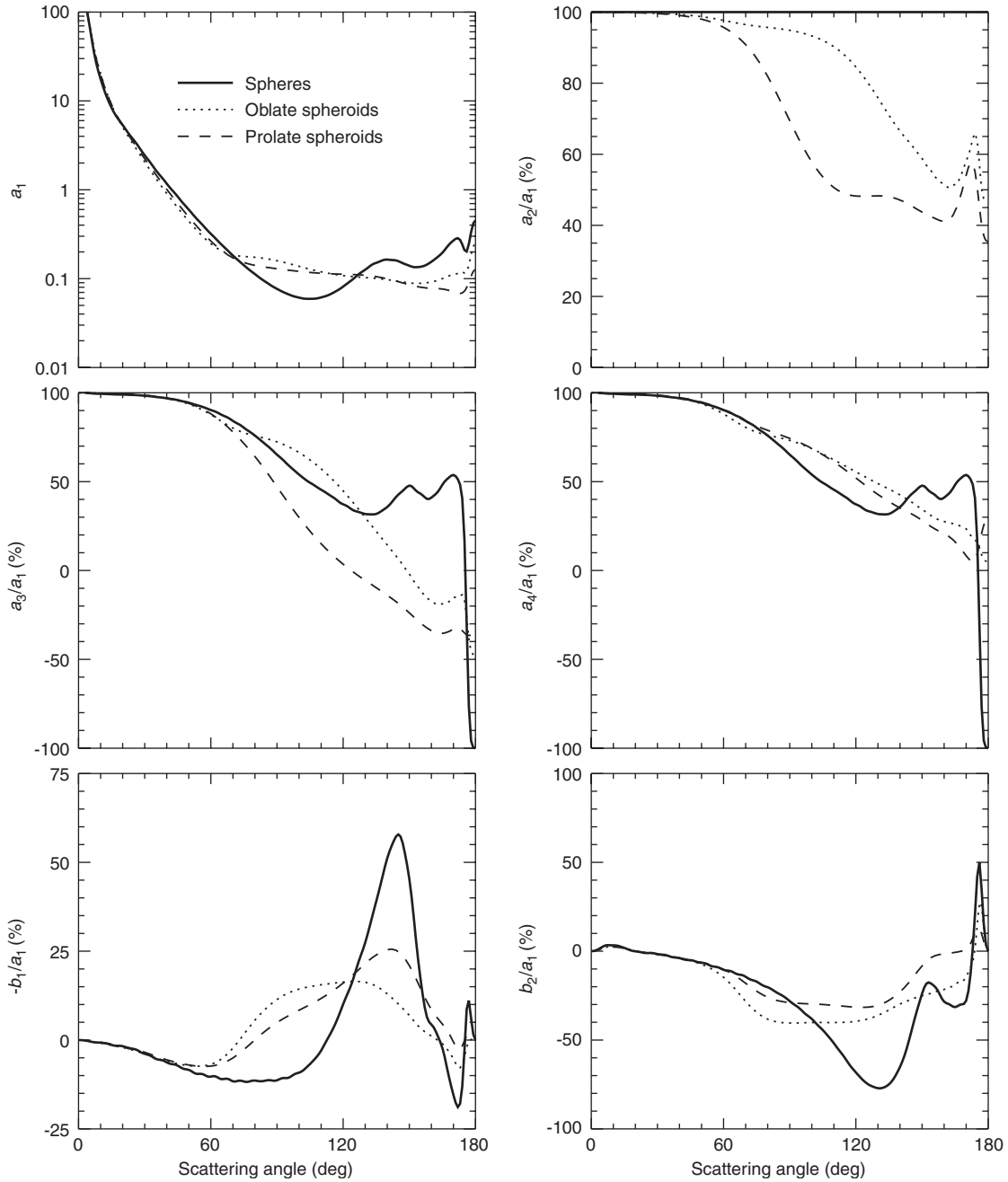

Fig. 1. Elements of the normalized Stokes scattering matrix versus scattering angle for polydisperse spheres (solid curves) and equiprobable shape mixtures of randomly oriented oblate (dotted curves) and prolate (dashed curves) spheroids with aspect ratios ranging from 1.2 to 2.4 in steps of 0.2. All curves were computed for the modified power law distribution of surface-equivalent-sphere radii at a wavelength of 1.88 μm and for the refractive index $1.2788 + 0.000317i$.

aspect-ratio distribution of oblate and prolate spheroids is smooth, featureless, and nearly flat at side-scattering angles. Importantly, it closely resembles those typically measured for natural ice crystals (see, e.g., the experimental phase function by Volkovitskiy et al. [42]). We thus conclude that phase functions of natural cirrus and contrail particles can be fairly well modeled using a wide aspect-ratio distribution of prolate and oblate spheroidal particles. In comparison to the ensemble-averaged phase function for spheroids, that for

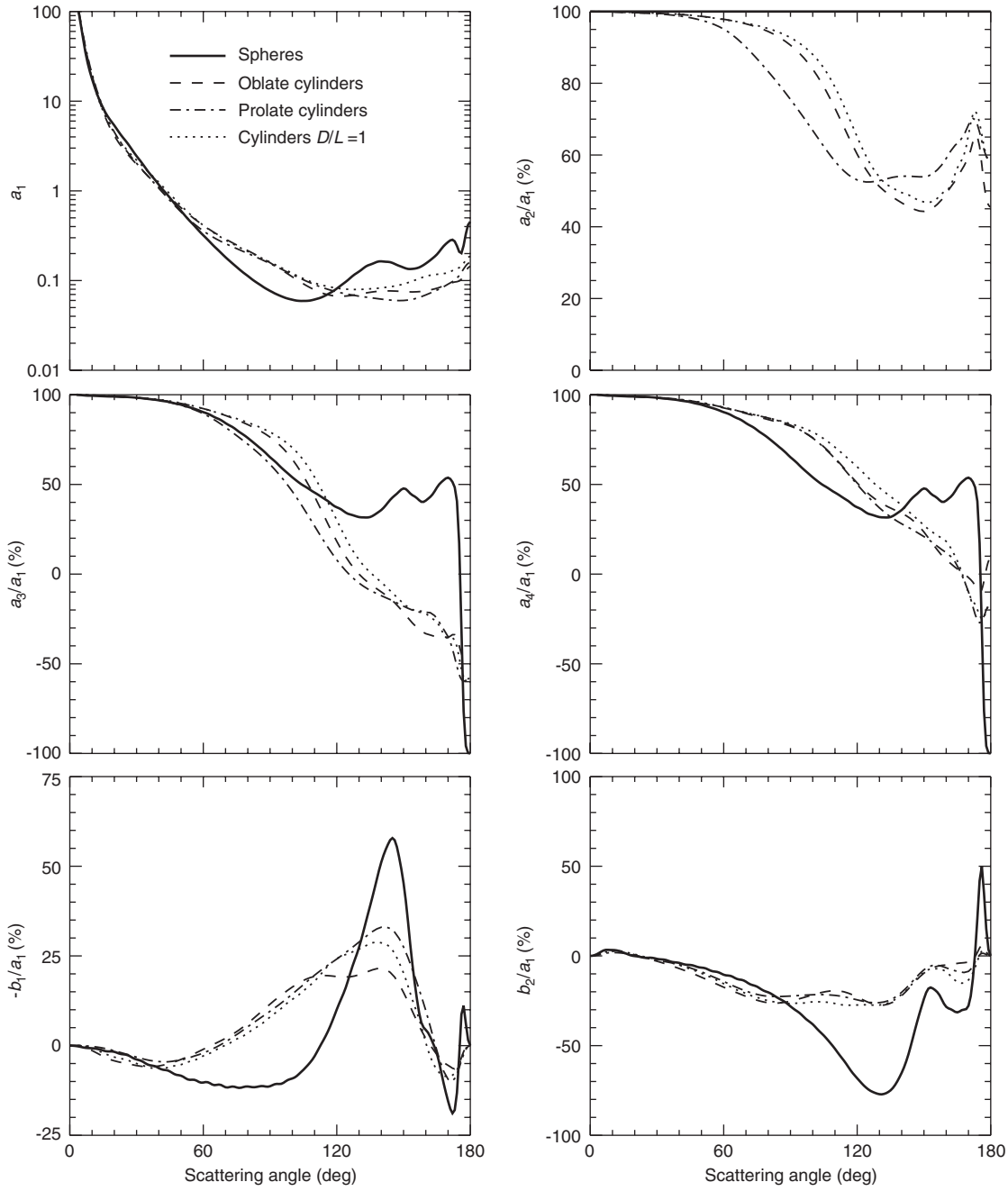

Fig. 2. Elements of the normalized Stokes scattering matrix versus scattering angle for polydisperse spheres (solid curves), compact cylinders with a diameter to length ratio $D/L = 1$ (dotted curves), and equiprobable shape mixtures of oblate (dashed curves) and prolate cylinders (dash-dotted curves) with the values of D/L or L/D ranging from 1.2 to 2.4 in steps of 0.2.

cylinders shows a relatively deeper minimum at side-scattering angles. However, it is still much closer to the phase function for spheroids than to that for spheres.

An important adverse implication of these results is that remote-sensing or in situ measurements of light scattering by cirrus clouds and contrails are unlikely to contain very specific information about the shape of real ice crystals. This conclusion has also been drawn in [37].

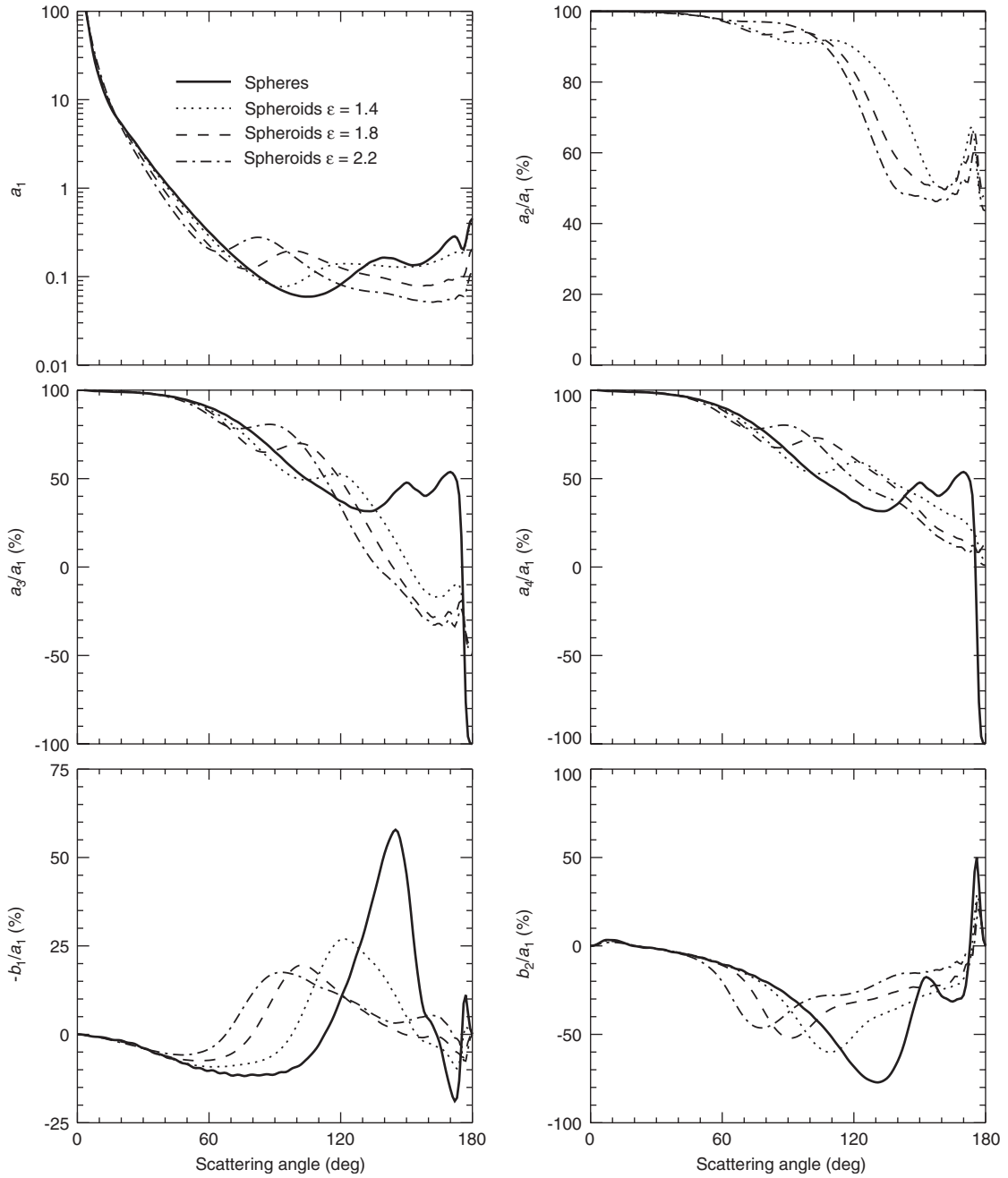

Fig. 3. Elements of the normalized Stokes scattering matrix versus scattering angle for polydisperse spheres and polydisperse, randomly oriented oblate spheroids with aspect ratios $\varepsilon = 1.4$, 1.8, and 2.2.

Table 1 demonstrates the differences in the integral photometric characteristics (the ensemble-averaged extinction, C_{ext}, scattering, C_{sca}, and absorption, C_{abs}, cross sections, the single-scattering albedo ϖ, and the asymmetry parameter g) between the nonspherical and spherical particles considered in this study. It is seen that spherical–nonspherical differences in the integral characteristics are significantly smaller than those in the scattering matrix elements, particularly for C_{abs}, ϖ, and g. This result suggests that the effect of particle shape on the radiative forcing caused by an optically thin cloud composed of small ice crystals can be relatively weak

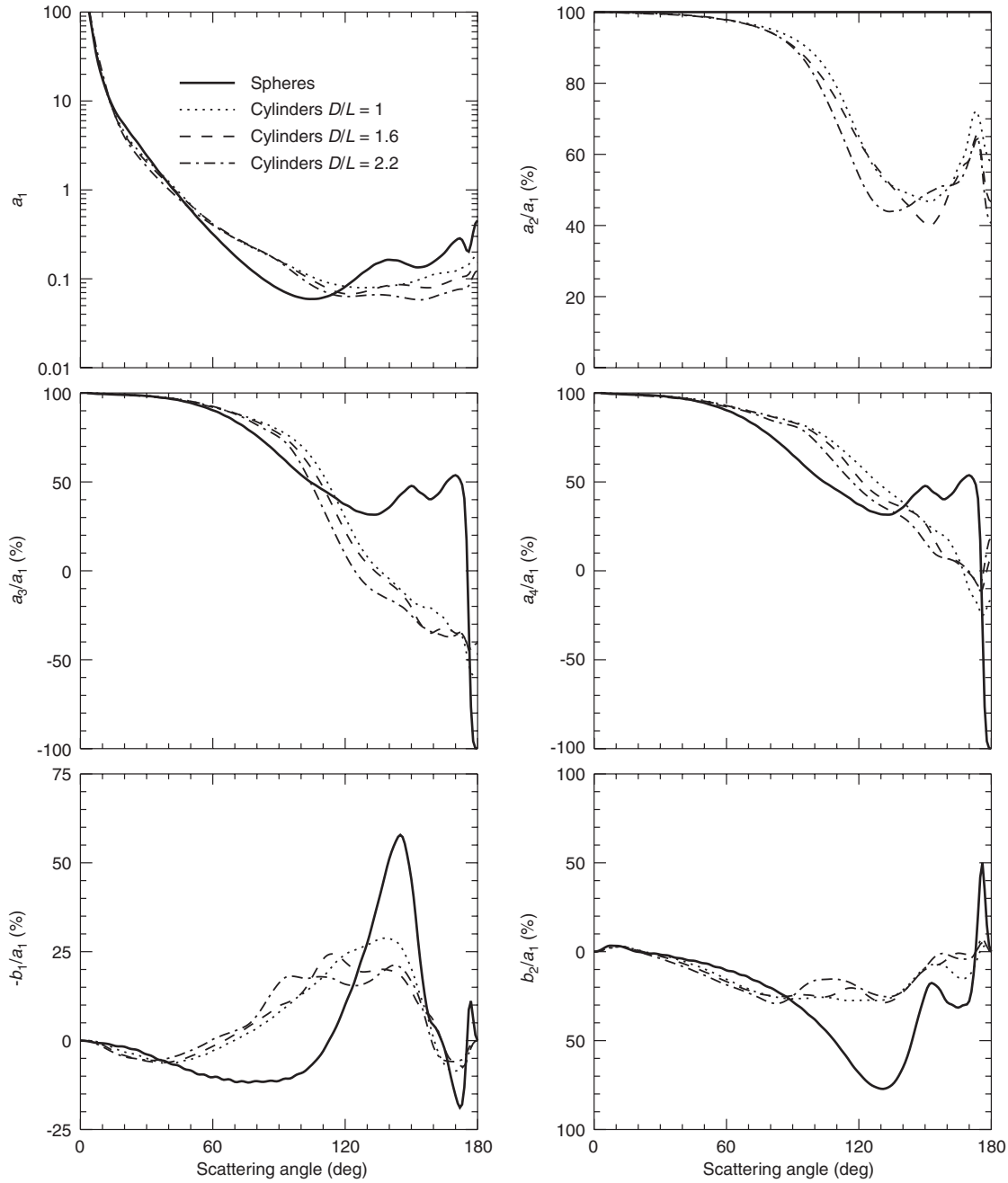

Fig. 4. Elements of the normalized Stokes scattering matrix versus scattering angle for polydisperse spheres and polydisperse, randomly oriented cylinders with diameter-to-length ratios 1, 1.6, and 2.2.

and can be rather accurately predicted by using the Lorenz–Mie theory, provided that the cloud optical thickness is already known (cf. [43,44]). The modeled asymmetry parameters fall in the range from 0.815 to 0.836 for all the cases considered in this study and are, thus, close to the average value $g \sim 0.824$ measured by Gerber et al. [45] for Arctic clouds.

Besides representing the single-scattering characteristics of ice crystals by a shape mixture of simple nonspherical particles such as spheroids and cylinders, a smooth and featureless phase function can also be

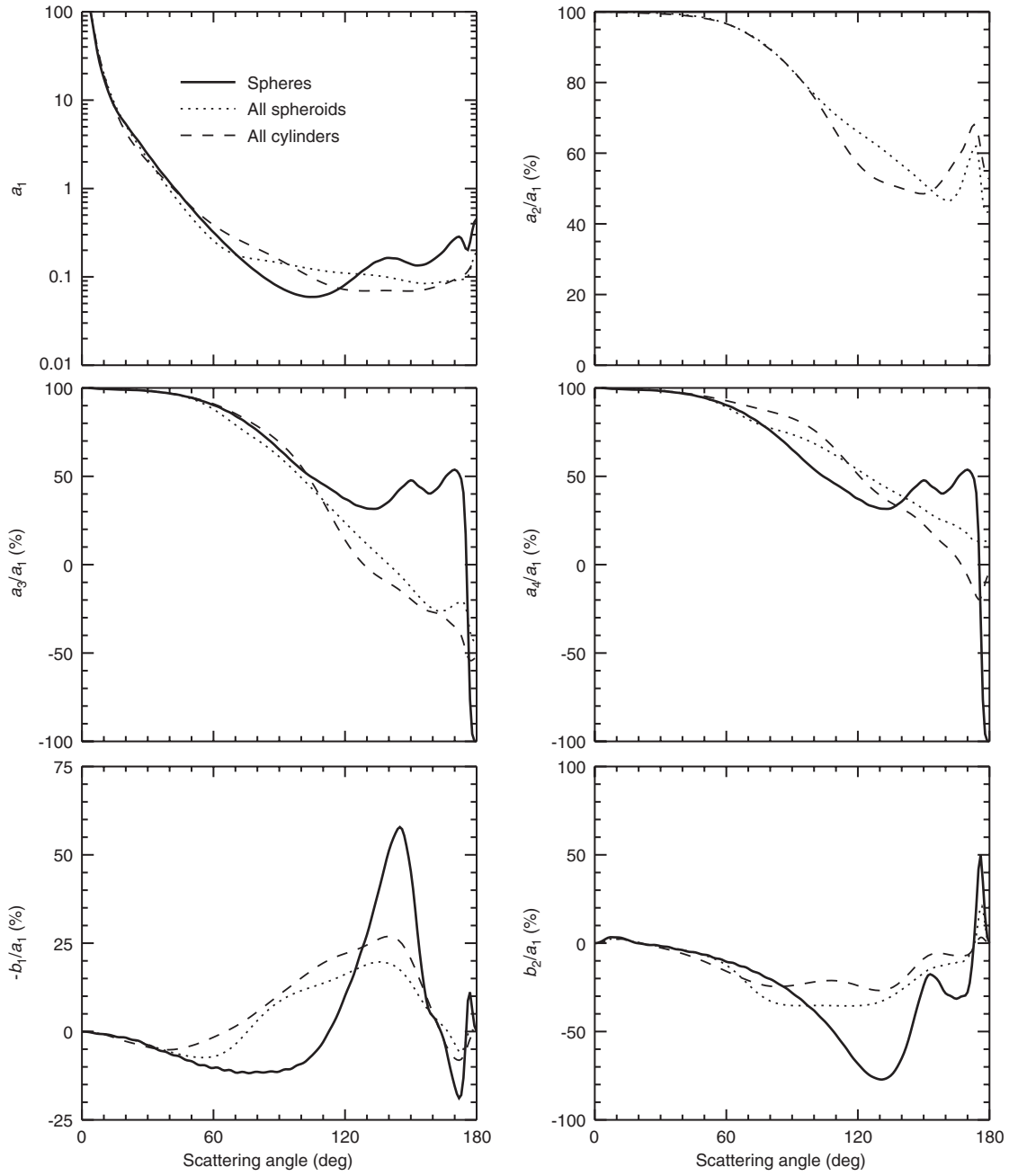

Fig. 5. Elements of the normalized Stokes scattering matrix versus scattering angle for equiprobable shape mixtures of all oblate and prolate spheroids (dotted curves) and all oblate and prolate cylinders (dashed curves) and for surface-equivalent spheres (solid curves).

generated by model scatterers in the form of randomized Koch fractals [46], ice crystals with microscopically rough surfaces [14], or ice particles with a large number of air–bubble inclusions [47–49]. Furthermore, Baran et al. [50] modeled the cirrus phase function using a simple analytical parameterization. All these theoretical developments need to be extensively tested using aircraft and satellite measurements. Our plan for future research is to apply the shape-averaged scattering matrix to the real RSP data and to compare the retrieval results with available in situ measurements.

Table 1
Integral optical characteristics of polydisperse randomly oriented ice crystals of different shapes

Shape	Spheres	Oblate spheroids	Prolate spheroids	All spheroids	Oblate cylinders	Prolate cylinders	All cylinders	Cylinders $D/L = 1$
C_{ext} (μm^2)	75.196	76.623	76.649	76.636	70.593	73.888	72.109	70.266
C_{sca} (μm^2)	74.522	76.015	76.028	76.022	70.078	73.368	71.589	69.716
C_{abs} (μm^2)	0.674	0.608	0.620	0.614	0.515	0.520	0.520	0.550
ϖ	0.991	0.992	0.992	0.992	0.993	0.993	0.993	0.992
g	0.825	0.829	0.834	0.832	0.830	0.836	0.832	0.815

Acknowledgment

We thank an anonymous referee for useful comments. This research was supported by the NASA Radiation Sciences Program managed by Hal Maring and by the NASA Glory project.

References

[1] Liou KN. Mon Weather Rev 1986;114:1167–99.
[2] Francis PN, Foot JS, Baran AJ. J Geophys Res 1999;104:31685–95.
[3] Gayet JF, Auriol F, Oshchepkov S, et al. Geophys Res Lett 1998;25:971–4.
[4] Yang P, Liou KN. Contr Atmos Phys 1998;71:223–48.
[5] Mishchenko MI, Rossow WB, Macke A, Lacis AA. J Geophys Res 1996;101:16973–85.
[6] Baran AJ, Watts PD, Francis PN. J Geophys Res 1999;104:31673–83.
[7] Foot JS. Q J R Meteorol Soc 1988;114:145–64.
[8] Francis PN. J Atmos Sci 1995;52:1142–54.
[9] Posse P, von Hoyningen-Huene W. Beitr Phys Atmos 1995;68:359–66.
[10] Crépel O, Gayet JF, Fournol JF, Oshchepkov S. Ann Geophys 1997;15:460–70.
[11] Wiscombe WJ, Mugnai A. Single scattering from nonspherical Chebyshev particles: a compendium of calculations. NASA Ref Publ 1157. Washington, DC: NASA; 1986.
[12] Bohren CF, Singham SB. J Geophys Res 1991;96:5269–77.
[13] Mishchenko MI, Travis LD, Kahn RA, West RA. J Geophys Res 1997;102:16831–47.
[14] Liou KN, Takano Y, Yang P, Gu Y. In: Lynch D, et al., editors. Cirrus. New York: Oxford University Press; 2001. p. 265–96.
[15] Mishchenko MI, Macke A. Appl Opt 1999;38:1626–9.
[16] Mishchenko MI, Hovenier JW, Travis LD, editors. Light scattering by nonspherical particles: theory, measurements, and applications. San Diego: Academic Press; 2000.
[17] Mishchenko MI, Travis LD, Lacis AA. Scattering, absorption, and emission of light by small particles. Cambridge: Cambridge University Press; 2002. (Available in the pdf format at 〈http://www.giss.nasa.gov/~crmim/books.html〉).
[18] Heymsfield AJ. J Atmos Sci 1986;43:851–5.
[19] Knollenberg RG, Kelly K, Wilson JC. J Geophys Res 1993;98:8639–64.
[20] Ackerman SA, Moeller CC, Strabala KI, et al. , Geophys Res Lett 1998;25:1121–4.
[21] Smith WL, Ackerman S, Revercomb H, et al. , Geophys Res Lett 1998;25:1137–40.
[22] Sassen K, Hsueh C-y. Geophys Res Lett 1998;25:1165–8.
[23] Mishchenko MI, Sassen K. Geophys Res Lett 1998;25:309–12.
[24] Iwasaki S, Tsushima Y, Shirooka R, et al. Geophys Res Lett 2004;31 L09103.
[25] Garrett TJ, Gerber H, Baumgardner DG, et al. , Geophys Res Lett 2003;30:2132.
[26] Hill SC, Hill AC, Barber PW. Appl Opt 1984;23:1025–31.
[27] Xu L, Ding J, Cheng AYS. Appl Opt 2002;41:2333–48.
[28] Baran AJ. Appl Opt 2003;42:2811–8.
[29] Lee Y-K, Yang P, Mishchenko MI, et al. Appl Opt 2003;42:2653–64.
[30] Kahn BH, Eldering A, Clough SA, et al. Geophys Res Lett 2003;30:1441.
[31] Jalava J-P, Taavitsainen V-M, Haario H, Lamberg L. JQSRT 1998;60:399–409.
[32] Volten H, Jalava J-P, Lumme K, et al. Appl Opt 1999;38:5232–40.
[33] Kahnert FM, Stamnes JJ, Stamnes K. J Opt Soc Am A 2002;19:521–31.
[34] Kahnert FM, Stamnes JJ, Stamnes K. JQSRT 2002;74:167–82.

[35] Nousiainen T, Vermeulen K. JQSRT 2003;79/80:1031–42.
[36] Kahnert M. JQSRT 2004;85:231–49.
[37] Nousiainen T, Kahnert M, Veihelmann B. JQSRT, in press, doi:10.1016/j.jqsrt.2006.02.038.
[38] Chowdhary J, Cairns B, Mishchenko M, Travis L. Geophys Res Lett 2001;28:243–6.
[39] Mishchenko MI, Cairns B, Hansen JE, et al. JQSRT 2004;88:149–61.
[40] Hansen JE, Travis LD. Space Sci Rev 1974;16:527–610.
[41] Mishchenko MI, Travis LD, Macke A. Appl Opt 1996;35:4927–40.
[42] Volkovitskiy OA, Pavlova LN, Petrushin AG. Izv USSR Acad Sci Atmos Oceanic Phys 1980;16:98–101.
[43] Lacis AA, Mishchenko MI. In: Charlson RJ, Heintzenberg J, editors. Aerosol forcing of climate. New York: Wiley; 1995. p. 11–42.
[44] Mishchenko MI, Lacis AA, Carlson BE, Travis LD. Geophys Res Lett 1995;22:1077–80.
[45] Gerber H, Takano Y, Garrett TJ, Hobbs PV. J Atmos Sci 2000;57:3021–34.
[46] Macke A, Mueller J, Raschke E. J Atmos Sci 1996;53:2813–25.
[47] Macke A, Mishchenko MI, Cairns B. J Geophys Res 1996;101:23311–6.
[48] Mishchenko MI, Macke A. JQSRT 1997;57:767–94.
[49] C.-Labonnote L, Brogniez G, Doutriaux-Boucher M, et al. Geophys Res Lett 2000;27:113–6.
[50] Baran AJ, Francis PN, Labonnote LC, Doutriaux-Boucher M. Q J R Meteorol Soc 2001;127:2395–416.